Tertiary boundary, which has been attributed to a major impact event. The strong evidence for an impact origin of the Bunyeroo ejecta also points to a cosmic source for its PGE signature.

The shales above and below the Bunyeroo ejecta horizon also show Ir and Pt enrichments (0.073–0.45 ppb Ir, 3.1–313 ppb Pt), suggesting postdepositional mobilization of Ir and Pt. Interelement ratios of the PGEs within the ejecta horizon from different sites are also quite variable, again suggesting postdepositional, low-temperature mobilization of these elements. Indeed, all green shale horizons in the Bunyeroo Formation that were analyzed, regardless of their stratigraphic position, have relatively high levels of Ir and other PGEs. The diagenetic origin of these anomalies is indicated by their association with enrichments in Cu-V-Zn-Co-Ni in thin, permeable green-colored reduced beds in a predominantly red bed sequence. A redox precipitation model similar to that invoked for red bed Cu-U-V deposits has been proposed to explain the PGE anomalies in the green shales [5].

In summary, the Bunyeroo ejecta is unique as the only known example of a widely dispersed, coarse-grained ejecta blanket that is, moreover, strongly linked to a known major impact structure. The marked Ir-PGE anomalies in the ejecta horizon provide support for the hypothesis that meteorite impact events can produce Ir anomalies in terrestrial sediments. The findings also indicate that Ir can be mobilized and concentrated in sediments by low-temperature diagenetic processes. The identification of ejecta horizons in sedimentary rocks therefore should be based on the coincidence of shock-metamorphic features in the detritus and clear Ir anomalies.

References: [1] Compston W. et al. (1987) *Aust. J. Earth Sciences, 34*, 435–445. [2] Gostin V. A. et al. (1986) *Science, 233*, 189–200. [3] Gostin V. A. et al. (1989) *Nature, 340*, 542–544. [4] Wallace M. W. et al. (1989) *Aust. J. Earth Sciences, 36*, 585–587. [5] Wallace M. W. et al. (1990) *Geology, 18*, 132–135. [6] Wallace M. W. et al. (1990) *Meteoritics, 25*, 161–165. [7] Wallace M. W. et al. (1990) *Mines and Energy Review, South Australia, 157*, 29–35. [8] Williams G. E. (1986) *Science, 233*, 200–203. [9] Williams G. E. (1987) *Search, 18*, 143–145.

OPTICAL AND TEM STUDY OF SHOCK METAMORPHISM FROM THE SEDAN TEST SITE.

A. J. Gratz, Lawrence Livermore National Laboratory, Livermore CA 94550, USA.

Thus far, detailed petrologic studies of shock metamorphism have been performed on samples recovered from laboratory experiments and on a few natural impactites. The loading history of these samples is quite different: In particular, laboratory experiments spend only a short time (<1 μs) at peak pressure, whereas natural impactites may have stress pulses from 0.1–1 ms. On the other hand, laboratory experiments have known stress histories; natural impactites do not. Natural samples are also subjected to thousands or millions of years of postshock annealing and/or weathering. A useful intermediate case is that of nuclear detonation. Stress pulses for these events can reach 0.1 ms or higher, and samples are obtained in pristine condition. All three types of loading produce stresses of hundreds of kilobars.

Samples studied were taken from the Sedan nuclear test site, and consist of a coarse-grained granodiorite containing quartz, K-feldspar, cordierite, and hornblende. Samples were studied optically in thin section, then were thinned with an ion mill and studied by transmission electron microscopy (TEM).

Optically, quartz and K-feldspar displayed numerous sets of planar deformation features (PDFs) identical to the nondecorated PDFs seen in laboratory samples and many natural impactites. Other minerals showed less distinct shock damage, with some fracturing visible in cordierite and hornblende.

TEM study showed that the PDFs in quartz and feldspar corresponded to densely packed wide transformation lamellae identical to those described in laboratory studies. The transformation lamellae in both minerals were amorphous, with no sign of high-pressure phases. In the case of K-feldspar only, narrow sublamellae extended outward from some wide lamellae. Quartz, which was more abundant and studied more extensively, contained no shock-induced dislocations. Some planar features were also seen in cordierite, but could not be identified due to rapid beam damage. No shock defects were seen in hornblende in TEM.

The shock-induced defects present at the Sedan site are very similar to those seen in shock recovery experiments, and also to those present at certain natural events (e.g., Meteor Crater). This suggests that shock deformation in quartz is not strongly dependent on shock pulse duration, and that laboratory recovery experiments are useful simulations of natural impact events. The lack of evidence for high-pressure phases along transformation lamellae is in agreement with past studies, and supports the idea that direct, solid-state amorphization occurs along transformation lamellae. Finally, no evidence was seen for decorated PDFs. Presumably decoration is due to postshock annealing or weathering. Further work should focus on processes that lead to decoration of transformation lamellae.

SIMULATED METEORITE IMPACTS AND VOLCANIC EXPLOSIONS: EJECTA ANALYSES AND PLANETARY IMPLICATIONS.

A. J. Gratz and W. J. Nellis, Lawrence Livermore National Laboratory, Livermore CA 94550, USA.

Past cratering studies have focused primarily on crater morphology. However, important questions remain about the nature of crater deposits. Phenomena that need to be studied include the distribution of shock effects in crater deposits and crater walls; the origin of mono- and polymict breccias; differences between local and distal ejecta; deformation induced by explosive volcanism; and the production of unshocked, high-speed ejecta that could form the lunar and martian meteorites found on the Earth. To study these phenomena, one must characterize ejecta and crater wall materials from impacts produced under controlled conditions.

New efforts at LLNL simulate impacts and volcanism and study resultant deformation. All experiments use the two-stage light-gas gun facility at LLNL to accelerate projectiles to velocities of 0.2 to 4.3 km/s, inducing shock pressures of 0.9 to 50 GPa. We use granite targets and novel experimental geometries to unravel cratering processes in crystalline rocks.

We have thus far conducted three types of simulations: soft recovery of ejecta, "frozen crater" experiments, and an "artificial volcano." In the first case, a projectile impacts a granite disk, jetting ejecta, which is gently recovered in a soft-foam fixture to minimize postejection deformation. In "frozen crater" experiments, a granite block is snugly embedded in a large Al block with a narrow entry tunnel for the projectile. The projectile, which deforms on impact, seals most of the ejecta in place, minimizing postimpact material movement and allowing study of the shocked material close to its preshock location. Volcanic simulations use impact projectiles on the back surface of preheated targets, producing stress waves that release at the front, unloading rapidly in much the same manner as a decompressing magma chamber.

Our ejecta recovery experiments produced a useful separation of impactites. Material originally below the projectile remained trapped there, embedded in the soft metal of the flyer plate. In contrast, material directly adjacent to the projectile was jetted away from the impact, producing an ejecta cone that was trapped in the foam recovery fixture. The high-speed ejecta showed no signs of shock metamorphism, only intense fracturing, including close intergranular fractures and some planar fracturing in feldspars. These effects are consistent with shock pressures of 5–10 GPa in the most damaged fragments while other fragments showed no significant internal damage. Material trapped in the flyer plate, in contrast, was highly shocked (10–40 GPa), with abundant planar deformation features (PDFs), amorphization, and micrometer-scale fracturing. Thus, we find that a significant component of crater ejecta shows no signs of strong shock; this material comes from the near-surface "interference zone" surrounding the impact site. This phenomenon explains the existence of unshocked meteorites on the Earth of lunar and martian origin. Impact of a large bolide on neighboring planets will produce high-speed, weakly shocked ejecta, which may be trapped by the Earth's gravitational field.

"Frozen crater" experiments show that the interference zone is highly localized; indeed, disaggregation does not extend beyond ~1.5 crater radii. A cone-shaped region extending downward from the impact site is completely disaggregated, including powdered rock (grain size <5 μm) that escaped into the projectile tube. Petrographic analysis of crater ejecta and wall material will be presented.

Finally, study of ejecta from 0.9- and 1.3-GPa simulations of volcanic explosions reveal a complete lack of shock metamorphism. The ejecta shows no evidence of PDFs, amorphization, high-pressure phases, or mosaicism. Instead, all deformation was brittle, with fractures irregular (not planar) and mostly intergranular. The extent of fracturing was remarkable, with the entire sample reduced to fragments of gravel size and smaller. Because the experimental shock stresses match those of the most energetic volcanic explosions, we conclude that explosive volcanism cannot produce shock features such as those seen at the K/T boundary. Instead, these features—similar to those seen in many meteor craters—must be the result of a large meteorite impact.

MELT PRODUCTION IN LARGE-SCALE IMPACT EVENTS: IMPLICATIONS AND OBSERVATIONS AT TERRESTRIAL CRATERS. Richard A. F. Grieve[1] and Mark J. Cintala[2], [1]Geophysics Division, Geological Survey of Canada, Ottawa, Ontario K1A 0Y3, [2]Code SN4, NASA Johnson Space Center, Houston TX 77058, USA.

The volume of impact melt relative to the volume of the transient cavity increases with the size of the impact event [1–3]. Here, we use the impact of chondrite into granite at 15, 25, and 50 km s^{-1} to model impact-melt volumes at terrestrial craters in crystalline targets and explore the implications for terrestrial craters; details of the model are given elsewhere [4,5].

Figure 1 illustrates the relationships between melt volume and final crater diameter D_R (i.e., after transient-cavity adjustments [5,6]) for observed terrestrial craters in crystalline targets; also included are model curves for the three different impact velocities.

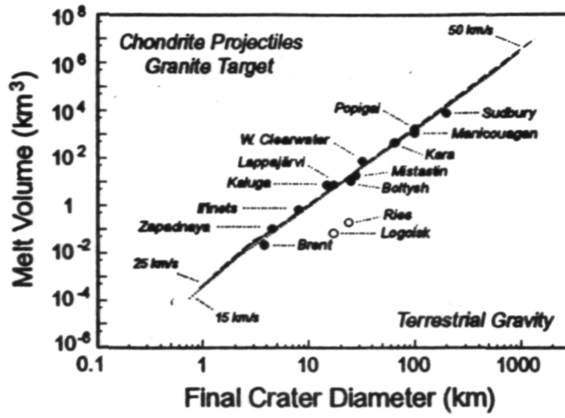

Fig. 1. Impact melt volumes as a function of final crater diameter for observed terrestrial craters and model curves. The slight breaks in slope at 3.1 km are due to application of the modification model of Croft [15].

One implication of the increase in melt volumes with increasing crater size (Fig. 1) is that the depth of melting will also increase (Fig. 2 and Fig. 5 in [6]). This requires that shock effects occurring at the base of the cavity in simple craters and in the uplifted peaks of central structures at complex craters record progressively higher pressures with increasing crater size, up to a maximum of partial melting (~45 GPa). Higher pressures cannot be recorded in the parautochthonous rocks of the cavity floor as they will be represented by impact melt, which will not remain in place. We have estimated maximum recorded pressures from a review of the literature [e.g., 7,8], using such observations as planar features in quartz and feldspar, diaplectic glasses of feldspar and quartz, and partial fusion and vesiculation, as calibrated with estimates of the pressures required for their formation (Table 1). Erosion complicates the picture by removing the surficial (most highly shocked) rocks in uplifted structures, thereby reducing the maximum shock pressures observed. In addition, the range of pressures that can be recorded is limited. Nevertheless, the data define a trend to higher recorded pressures with crater diameter (Table 1), which is consistent with the implications of the model.

TABLE 1. Estimates of maximum recorded shock pressures in the center of craters formed in crystalline targets.

Crater	D_R (km)	Pressure (GPa)	Notes
Rotmistrovka*	2.5	~25	
Brent*	3.8	<25	
Logoisk	20	~30	
Boltysh	25	35-40	
Mistastin	28	>30-35	Eroded
Slate Islands	30	>20	Eroded
W. Clearwater	32	>30-35	Eroded
Araguainha	40	>32	Eroded
Charlevoix	54	>25	Eroded
Kara	60	>35-40	Eroded
Puchezh-Katunki	80	40-45	
Manicouagan	100	40-45	Eroded
Popigai	100	40-45	

Better constrained estimates are shaded.

* Simple craters; all others are complex.